

# Proton-proton elastic scattering; Landshoff contributions in the diquark model

Rainer Jakob

*Fachbereich Physik, Universität Wuppertal,*

*D-42097 Wuppertal, Germany\**

(October 29, 2018)

## Abstract

Independent multiple scattering ('Landshoff') contributions to proton-proton elastic scattering at wide angles are calculated in the quark-diquark model. Results confirm previous observations about the magnitude of these contributions. The use of the quark-diquark model extends the applicability of perturbative QCD calculations down to lower values of momentum transfer substantially.

12.38.Bx, 13.85.Dz

Typeset using REVTeX

---

\*Supported by the Deutsche Forschungsgemeinschaft

## I. INTRODUCTION

Despite tiny cross sections and corresponding difficulties for experimentalists, exclusive processes are the natural approach to study the composite character of hadrons. For large momentum transfer the wave functions deeply penetrate each other without producing a torrent of secondary particles in the final state. Thus compositeness is probed without destroying the observed configuration.

Perturbative Quantum Chromodynamics (PQCD) in the framework of the hard scattering picture (HSP) [1–3] is the generally accepted theory to describe exclusive processes at large momentum transfer. Factorization of long- and short-range physics, the basic assumption of the HSP, is reflected in the fact that exclusive quantities are expressed as convolutions of process independent distribution amplitudes (DA) with a perturbative, hard amplitude for the scattering of nearly collinear constituents.

The applicability of PQCD at intermediate momentum transfer of a few GeV, where experimental data are available, is a matter of passionate controversy [4,5]. The overall momentum transfer in the process has to be shared between the constituents in order to align them suitably for subsequent hadronization into the final state. Consequently, the corresponding strong coupling in parts of the process may become too large for reasonable use of perturbative methods. In particular, this is the case, when the momentum of a hadron is unequally shared between its constituents.

Hard elastic proton-proton scattering will certainly be a cornerstone of investigations about the hadronic structure. Unfortunately, the relative complexity of the scattering of composite objects off each other — even if one only takes into account the valence quark Fock states and diagrams on the Born-level — has prevented the complete cross sections from being calculated up to now. The complexity is revealed in the huge number of diagrams to be calculated ( $\simeq$  in the order of 100,000), as well as in the occurrence of pinch-singularities, which are closely related to the existence of independent, multiple scattering (‘Landshoff’ [6]) contributions.

In a novel treatment of the ‘Landshoff’ mechanism in elastic proton-proton scattering Botts and Sterman [7,8] pointed out the need for taking into account transverse momenta in the HSP, which have been neglected before. The role of transverse momenta in the ‘Landshoff’ mechanism is manifold: The energy dependence of the cross section is understandable when one takes into consideration the scaling behavior of momentum components transverse to the scattering plane. Also, as has been shown in [7], the way transverse momenta are dealt with is decisive in deriving a factorized formula for the scattering amplitude. Soft, gluonic (‘Sudakov’ [9]) corrections have been resummed by the use of renormalization group techniques. Here, the transverse separation between constituents (i.e. the conjugate variable of the transverse momentum) acts as an infrared cut-off and provides finiteness of the results of loop-integrations. The resulting ‘Sudakov’ factor leads to a suppression of the scattering amplitude and, thus, affects the probability for a proton to contribute to elastic scattering, depending on the transverse separation between the constituents of the proton.

The work of Botts and Sterman [7] about the ‘Landshoff’ mechanism initiated an approach [10,11], which is addressed to refute the above mentioned criticism [4,5] of the applicability of perturbative methods by modifying and improving on the HSP. The basic idea, which has been demonstrated for the calculation of electromagnetic form factors in [10,11], is to take into account the transverse momenta consistently also in the hard scattering amplitude, where it still had been neglected in [7,8]. Dangerous, soft integration regions, where the validity of perturbative formulas becomes doubtful, are damped by the ‘Sudakov’ corrections. Thus, self-consistency of the perturbative calculation is achieved in the modified HSP even for momentum transfers as low as a few GeV. Here, self-consistency is meant in the sense that the bulk of the results is derived with reasonable small values for the strong coupling. Additionally, the non-perturbative, intrinsic transverse structure turns out to be important, as it strengthens the suppression of soft regions. On the other hand, it provides a substantially smaller perturbative result [12,13].

In the course of these developments the role of transverse momenta in hard scattering processes, and correspondingly the transverse structure of hadrons, has received a lot of

attention [7,8,10,11,14–17].

In the present paper the ‘Landshoff’ contributions of proton-proton elastic scattering at wide angles are calculated within a model in which the proton is considered as a quark-diquark system. The treatment of two correlated quarks as an effective diquark is a possibility to cope with non-perturbative effects still present in the kinematic range of interest. A systematic study of photon-proton reactions has been carried out in the quark-diquark model: form factors in the space-like and time-like region, real and virtual Compton scattering, two-photon-annihilations into proton-antiproton as well as photoproduction of mesons [18–20].

The motivation for the present investigation in the quark-diquark model is the hope for an improvement of the applicability of the HSP down to lower energies, compared to observations made by Botts [8] in the pure quark picture. On the other hand, the reduction of complexity (two constituents instead of three to deal with in the valence Fock states) results in a technical simplification, which is not dramatic for the ‘Landshoff’ contributions, but might become decisive for a future attempt to calculate all HSP diagrams (several 100’s of diagrams instead of several 100,000’s).

The paper is organized as follows. In Sec. II the elements of the quark-diquark model necessary for the present calculation are briefly introduced. The mechanism of independent scatterings is envisaged in Sec. III, gluonic ‘Sudakov’ corrections in the context of the quark-diquark model are discussed and a factorized formula for helicity amplitudes for the ‘Landshoff’ contribution to elastic proton-proton scattering at wide angles is given. Sec. IV contains a discussion of numerical results. Conclusions are given in Sec. V.

## II. THE QUARK-DIQUARK MODEL

The basic assumption of the diquark model is the clustering of two of the three valence quarks in a baryon on an intermediate energy scale, which allows to describe these two quarks, including correlation effects, as an effective particle, the diquark. Hence, some non-

perturbative effects still present on this intermediate scale are taken into account. The coupling of spin-1/2 and flavor (isospin-1/2) wave functions of two quarks leads to scalar and vector diquark wave functions. The symmetry of proton wave functions requires the spin and the flavor parts of the diquark wave functions to have the same symmetry. In this paper only the scalar sector of the model is considered, which is known to give rise to the bulk of numerical results. The vector sector is essential for spin effects, but may be negligible for cross section results. The quark-scalar diquark (S) Fock state contribution to the proton state as a function of the usual longitudinal momentum fraction  $x$  and transverse momentum  $\vec{k}_\perp$  of the quark with respect to the proton's momentum  $P$  is

$$|P, \lambda\rangle_{Sq} = \int \frac{dx d^2k_\perp}{16\pi^3 \sqrt{x x'}} \Psi_S(x, \vec{k}_\perp) |S(x', \vec{k}'_\perp) u_\lambda(x, \vec{k}_\perp)\rangle \quad , \quad (1)$$

where  $x' = 1 - x$  is the longitudinal momentum fraction of the diquark and  $\vec{k}'_\perp$  it's transverse momentum.

The dynamical content of the model is invoked by treating the diquark as an elementary particle with corresponding Feynman rules for the propagator of a scalar diquark and the gluon diquark vertex respectively as

$$\text{propagator} : \quad \frac{i}{p^2 - m_S^2 + i\varepsilon} \delta_{ij} \quad \quad SgS - \text{vertex} : \quad i g_s t^a (p_1 + p_2)_\mu \quad , \quad (2)$$

where  $g_s = \sqrt{4\pi\alpha_s}$  is the QCD coupling,  $i, j$  are color indices and  $t^a = \lambda^a/2$  are the Gell-Mann color matrices. Diquarks are in an antitriplett color state, as is necessary to form a color neutral baryon out of a diquark and a single colored quark. The composite nature of the diquarks is taken into account by the introduction of phenomenological vertex functions which may be parametrized as

$$F_S(Q^2) = \delta_S \left( \frac{Q_S^2}{Q_S^2 + Q^2} \right) \quad \delta_S = \begin{cases} 1 & \text{for } Q^2 < Q_S^2 \\ \alpha_s(Q^2)/\alpha_s(Q_S^2) & \text{for } Q^2 \geq Q_S^2 \end{cases} \quad , \quad (3)$$

where  $Q^2$  is the modulus of the squared momentum of the gluon entering the vertex. This form is chosen to ensure the diquark model to evolve into the pure quark HSP in the limit  $Q^2 \rightarrow \infty$ .

### III. ‘LANDSHOFF’ CONTRIBUTIONS TO pp ELASTIC SCATTERING

#### A. The ‘Landshoff’ mechanism

Independent scatterings in exclusive processes occur when pairs of constituents accidentally scatter by the same angle. In this case the momentum transfer has not to be distributed in the hadrons any further in order to guarantee nearly collinear outgoing constituents, which are able to hadronize again; the outgoing constituents are already suitably aligned by chance in this special kinematical situation. This results in a lower minimal number of gluons to be exchanged as compared to the minimal number of gluons necessary in a general HSP diagram. Consequently, with increasing energy ‘Landshoff’ contributions do not decrease according to ‘dimensional counting’ rules [21], but a bit slower.

This, so-called, ‘Landshoff effect’ may be explained by the observation that components of momenta transverse to the scattering plane exhibit a different scale dependence as compared to the other components. The reason for this behavior is that independent scatterings can be spatially separated in the direction transverse to the scattering plane. On the contrary, with respect to directions in the scattering plane the independent hard scatterings are restricted to take place in a small region, the extension of which is invers proportional to the center of mass energy, i.e. proportional to  $1/Q$ .

The scaling behavior may be illustrated by considering the kinematics of a ‘Landshoff’ process. In the quark-diquark model two types of diagrams contribute as indicated in Fig. 1. Fig. 1a correspond to a independent quark-quark and a diquark-diquark scattering, whereas Fig. 1b shows two independent quark-diquark scatterings. The kinematics of Fig. 1a will be discussed in the following, kinematics of Fig. 1b can be inferred from the former by substitutions. Neglecting masses and choosing the scattering plane to be the  $(z-x)$ -plane the momenta in the hadronic center of mass system are given as

$$\begin{aligned}
 P_1 &= (Q, 0, 0, Q) & P_2 &= (Q, 0, 0, -Q) \\
 P_3 &= (Q, Q \sin \theta, 0, Q \cos \theta) & P_4 &= (Q, -Q \sin \theta, 0, -Q \cos \theta) \quad .
 \end{aligned}
 \tag{4}$$

The internal quark momenta (see Fig. 1a) may be parametrized as

$$\begin{aligned}
\vec{p}_1 &= x_1 \vec{P}_1 + \vec{k}_1 &\Rightarrow p_1 &= (x_1 Q + \sigma_1/Q, & k_{1x} &, \\
\vec{p}_2 &= x_2 \vec{P}_2 + \vec{k}_2 &\Rightarrow p_2 &= (x_2 Q + \sigma_2/Q, & k_{2x} &, \\
\vec{p}_3 &= x_3 \vec{P}_3 + \vec{k}_3 &\Rightarrow p_3 &= (x_3 Q + \sigma_3/Q, & x_3 Q \sin \theta + k_{3x} &, \\
\vec{p}_4 &= x_4 \vec{P}_4 + \vec{k}_4 &\Rightarrow p_4 &= (x_4 Q + \sigma_4/Q, & -x_4 Q \sin \theta + k_{4x}, k_{4y}, & -x_4 Q \cos \theta + k_{4z}) . \quad (5)
\end{aligned}$$

Internal momenta of the diquarks,  $p'_i$ , have an analogous form. In the energy components extra terms,  $\sigma_i/Q$ , are included to allow for ‘on-shellness’ of the quarks. Assuming all transverse momenta (and, therefore, all  $\sigma_i$  induced in the energy components by the transverse momenta) to be small compared to  $Q$ , the four momentum conservation for the quark-quark scattering reads

$$\delta^{(4)}(p_1 + p_2 - p_3 - p_4) \simeq \frac{\delta(x_1 - x_3) \delta(x_2 - x_4) \delta(x_1 - x_2)}{2Q^3 \sin \theta} \delta(k_{1y} + k_{2y} - k_{3y} - k_{4y}) \quad . \quad (6)$$

All longitudinal momentum fractions,  $x_i$ , involved in the quark-quark scattering are constrained to be equal. This is characteristic for the special kinematical situation in the ‘Landshoff’ mechanism. The usual, hadronic Mandelstam variables take the values  $s = 4Q^2$  and  $t = -2Q^2(1 - \cos \theta)$ . Their partonic equivalents are approximated by  $\hat{s} \simeq x^2 s$ ;  $\hat{t} \simeq x^2 t$ ;  $\hat{s}' \simeq x'^2 s$ ;  $\hat{t}' \simeq x'^2 t$ . Hence, both partonic scattering angles are equal to the scattering angle of the hadronic process and, therefore, aligned constituents keep aligned during the scattering process. The power of  $Q$  in the denominator of Eq. (6) is determined by the scaling behavior of the energy component and the two momentum components in the scattering plane. The momentum conservation transverse to the scattering plane (here: in the  $y$ -direction) is independent of the  $Q$ -scale, as can be seen from Eq. (6).

The energy dependence of the hadronic scattering amplitude for the ‘Landshoff’ process may now be summed up as

$$M_{fi} \sim Q^{-3} F^2(Q^2) \quad (\text{modulo logs}) \quad . \quad (7)$$

The factor  $Q^{-3}$  originates from the momentum conservation for the quark-quark scattering, Eq. (6). The momentum conservation for the diquark-diquark scattering has not to be

considered separately, because the overall (hadronic) momentum conservation automatically implies it, if the one for the quark-quark scattering holds. The second factor,  $F^2(Q^2)$ , stems from the diquark-diquark scattering, whereas the quark-quark scattering only depends on the scattering angle. The hadronic wave functions depend only logarithmically on the energy scale. Consequently, the ‘Landshoff’ contributions to the differential cross section for elastic proton-proton scattering in the quark-diquark description behave as

$$\frac{d\sigma}{dt} = f(s/t) \cdot s^{-5} \cdot F_S^4(Q^2) \quad \longrightarrow \quad f(s/t) \cdot s^{-9} \quad \text{for } s \rightarrow \infty \quad . \quad (8)$$

This has to be compared with the predictions from the ‘dimensional counting’ rules: Inserting one additional hard gluon in a ‘Landshoff’ diagram converts it into a HSP diagram. Then, there are no longer two separate momentum conservations, the  $Q^{-3}$ -dependence caused by the  $\delta$ -function is dropped. But instead, the additional elements of the Feynman diagram give rise to a factor  $Q^{-4}$ . (The insertion of a virtual gluon between two quark lines, for example, introduces two quark propagators, two quark-gluon vertices, and the gluon propagator, which asymptotically scale like  $\{Q^{-1}\}^2$ ,  $\{Q^0\}^2$ , and  $\{Q^{-2}\}^0$ , respectively.) Thus, the amplitude for a general HSP diagram behaves as  $Q^{-4} F_S^2(Q^2)$ , which leads to an  $s^{-10}$ -behavior for the differential cross section asymptotically.

## B. ‘Sudakov’ corrections

The leading radiative corrections to elastic proton-proton scattering are similar in form to vertex loop-corrections. For the case of QED Sudakov [9] has shown that the coincidence of ‘soft’ and ‘collinear’ divergencies in vertex corrections typically leads to double logarithmic terms. Infrared divergencies are regulated in these calculations by allowing for small virtualities of external fermion lines. A similar form has been derived for QCD vertex corrections [22], where the non-abelian character of QCD is reflected in the appearance of  $\ln(\ln(q^2/m^2))$  terms. Higher order of loop-corrections may be taken into account by exponentiating single loop results [23].



In the quark-diquark picture ‘Sudakov’ corrections to proton-proton scattering are very similar to the corrections in the pion-pion case, due to the fact, that diquarks carry the same color as antiquarks. In Fig. 2 two types of gluonic corrections are indicated. In axial gauge leading logarithms are given by corrections of type I, which may be factorized into the wave functions. Corrections of type II, which are non-factorizable, result in non-leading logarithms.

A single-loop calculation in leading logarithm approximation has been carried out for gluonic corrections to the proton wave function in the quark-diquark model. Exponentiating the result to account for higher loops (but not for non-leading logarithms) leads to a suppression factor

$$\exp[-S(x, b, Q)] = \exp[-s(x, b, Q) - s(1-x, b, Q)] \quad (9)$$

with

$$s(x, b, Q) = \frac{C_F}{2\beta_1} \left\{ \ln\left(\frac{x\sqrt{2}Q}{\Lambda_{QCD}}\right) \ln\left[\frac{\ln(x\sqrt{2}Q/\Lambda_{QCD})}{-\ln(b\Lambda_{QCD})}\right] - \ln\left(\frac{x\sqrt{2}Q}{\Lambda_{QCD}}\right) - \ln(b\Lambda_{QCD}) \right\} \quad , \quad (10)$$

where  $C_F = 4/3$  is the color factor and  $\beta_1 = (11 - 2/3n_f)/4$ . Throughout this paper  $n_f = 3$  and  $\Lambda_{QCD} = 200$  MeV is used. The result in Eq. (9) and Eq. (10) is equal to the correction for a pion wave function and, hence, confirms that ‘Sudakov’ corrections depend on color and not on spin.

An essential point in Eq. (10) is the appearance of the ‘impact parameter’  $b$ , which acts as an infrared cut-off. The physical intuitive picture is that the proton is viewed as a color dipole, formed by a quark and a diquark. Therefore, the momentum range of soft gluons, contributing to the corrections, is limited: The upper limit is given by the large component of the quark (diquark) momentum, i.e.  $x\sqrt{2}Q$  or  $x'\sqrt{2}Q$ , respectively. Harder gluons are considered as higher order corrections to the hard scatterings and not as a part of the soft ‘Sudakov’ corrections. The lower limit is induced by the inverse of the transverse separation of the color charges,  $1/b$ . Gluons with wave lengths larger than the dipole parameter  $b$

effectively ‘see’ a color neutral object and decouple from the proton. The larger the range of momenta between these two limits for a given configuration, the stronger is the suppression by the ‘Sudakov’ factor. For a very small transverse separation the infrared limit  $1/b$  is close to the upper limit; there is no suppression. A larger value of  $b$  results in a strong suppression. In Fig. 3 the ‘Sudakov’ factor, Eq. (9) is displayed for a given value of  $x = 0.5$  and different values of  $Q$ . Clearly the suppression tends to force  $b$  to zero for increasing  $Q$ .

Although the tendency of the ‘Sudakov’ corrections to keep colored constituents together is somehow similar to the effect of confinement, it should be emphasized, that Eq. (9) and Eq. (10) are entirely perturbative. The ‘Sudakov’ factor describes the fact, that the probability for a scattering process to take place in the exclusive channel is decreasing with increasing spatial separation. It should not be mixed up with the non-perturbative effect of confinement.

Resummation techniques based on renormalization group equations have been developed to take into account leading as well as non-leading logarithms to all orders [24,25,7]. Working in a phenomenological model like the quark-diquark model, it seems reasonable to take a pragmatic point of view: Only the exponentiated, leading-logarithmic corrections of Eq. (9) and Eq. (10) are considered in the present calculations. Tacitly it is assumed that the neglect of non-leading corrections is an acceptable approximation, as is indicated by the results of resummations in the pure quark picture.

Mueller [26] and Botts and Sterman [7] have shown, for the cases of pion-pion and proton-proton scattering in the pure quark picture, that gluonic ‘Sudakov’ corrections to the ‘Landshoff’ contributions shift the power of the asymptotic behavior near to the ‘dimensional counting’ expectation. Their arguments can readily be transferred to the present case of proton-proton scattering viewed in the diquark model: Assuming, for the moment, that the only  $b$ -dependence of the amplitude is contained in the ‘Sudakov’ factors Eq. (9) of the four proton wave functions, the integration over the  $b$ -space can be estimated by insertion of Eq. (10) and the use of a saddle point approximation in the form

$$\int_0^\infty db \exp[-4S(x, b, Q)] \simeq \frac{\sqrt{2\pi}}{\Lambda_{QCD}} \frac{\sqrt{c}}{1+c} \sqrt{\ln(\sqrt{2xx'Q}/\Lambda_{QCD})} \left(\frac{\sqrt{2xx'Q}}{\Lambda_{QCD}}\right)^{-c \ln(\frac{1+c}{c})}, \quad (11)$$

where

$$c = \frac{4C_F}{\beta_1} = \frac{64}{27}, \quad b_{sp} = \frac{1}{\Lambda_{QCD}} \left(\frac{\sqrt{2xx'Q}}{\Lambda_{QCD}}\right)^{-\frac{c}{1+c}}. \quad (12)$$

Thus, the leading power of  $Q$ , induced in the amplitude by the ‘Sudakov’ corrections, is given by  $-c \ln(1 + 1/c) = -0.83$ . Consequently the power of  $s$  in Eq. (8) for the differential cross section is changed to  $-9.83$ , which will be not distinguishable experimentally from a power  $-10$  in the foreseeable future.

### C. Hadronic helicity amplitudes

Using Eq. (1) for the proton helicity states a matrix element for the hadronic process reads

$$\begin{aligned} \langle P_3 P_4 | T | P_2 P_1 \rangle &= \int \prod_{i=1}^4 \frac{dx_i d^2 k_{\perp i}}{16\pi^3 \sqrt{xx'}} \Psi_S^*(\vec{p}_3) \Psi_S^*(\vec{p}_4) \Psi_S(\vec{p}_2) \Psi_S(\vec{p}_1) \\ &\times \left\{ \langle q_3 q_4 | \hat{T} | q_1 q_2 \rangle \langle S_3 S_4 | \hat{T}' | S_2 S_1 \rangle + \langle q_3 S_4 | \hat{T} | q_2 S_1 \rangle \langle S_3 q_4 | \hat{T}' | S_2 q_1 \rangle \right\} \end{aligned} \quad (13)$$

where  $\hat{T}$  and  $\hat{T}'$  denote the two partonic transition matrices of the independent scatterings.  $S_i$  and  $q_i$  symbolize the  $i$ -th scalar diquark and the  $i$ -th quark, respectively. The momenta of hadrons,  $P_i$ , quarks,  $p_i$ , and diquarks,  $p'_i$ , are defined as indicated in Eq. (4) and Eq. (5). Reminding the relation between transition matrix elements and Feynman amplitudes  $T_{fi} = i(2\pi)^4 \delta^{(4)}(\vec{P}_f - \vec{P}_i) M_{fi}$  and the fact that momentum conservation for each of the independent partonic scatterings implies the overall hadronic momentum conservation, Eq. (6) leads to

$$\begin{aligned} M_{fi}(s, t) &= \frac{i}{(2\pi)^8} \frac{1}{2^5 Q^3 \sin \vartheta} \int_0^1 \frac{dx}{x^2 x'^2} \int \prod_{i=1}^4 d^2 k_{\perp i} \delta(k_{1y} + k_{2y} - k_{3y} - k_{4y}) \\ &\left\{ \Psi_S^*(x, \vec{k}_{\perp 4}) \Psi_S^*(x, \vec{k}_{\perp 3}) \hat{M}_{qq;qq}(x, \hat{s}, \hat{t}) \hat{M}'_{SS;SS}(x, \hat{s}', \hat{t}') \Psi_S(x, \vec{k}_{\perp 2}) \Psi_S(x, \vec{k}_{\perp 1}) \right. \\ &\left. + \Psi_S^*(x', -\vec{k}_{\perp 4}) \Psi_S^*(x, \vec{k}_{\perp 3}) \hat{M}_{qS;qS}(x, \hat{s}, \hat{t}) \hat{M}'_{Sq;Sq}(x, \hat{s}', \hat{t}') \Psi_S(x', -\vec{k}_{\perp 2}) \Psi_S(x, \vec{k}_{\perp 1}) \right\}, \end{aligned} \quad (14)$$

where  $\hat{M}$  and  $\hat{M}'$  denote the partonic amplitudes. Following the basic idea of Botts and Sterman [7] a factorized formula can be derived, when the remaining  $\delta$ -function in Eq. (14), which is caused by the conservation of momentum components transverse to the scattering plane, is expressed by it's Fourier transform

$$\delta(k_{1y} + k_{2y} - k_{3y} - k_{4y}) = \frac{1}{2\pi} \int_{-\infty}^{\infty} db e^{i b \cdot (k_{1y} + k_{2y} - k_{3y} - k_{4y})} \quad . \quad (15)$$

The terms  $e^{i \cdot k_{iy}}$  may be reabsorbed together with momentum integrations over the  $k_{iy}$  by the definition of wave functions in the form

$$\tilde{\Psi}(x, k_{ix}, b) \equiv \int \frac{dk_{iy}}{2\pi} \Psi_S(x, \vec{k}_{\perp, i}) e^{-i b \cdot k_{iy}} \quad . \quad (16)$$

These wave functions  $\tilde{\Psi}(x, k_{ix}, b)$  are the Fourier transforms of the old ones,  $\Psi_S(x, \vec{k}_{\perp, i})$  with respect to the  $y$ -component. Eq. (16) defines the parameter  $b$  to be the conjugate variable to the transverse momentum  $k_{iy}$ . Hence, as was mentioned above,  $b$  may be associated with the separation of quark and diquark in the proton in the  $y$ -direction. The effects of soft gluonic 'Sudakov' corrections are taken into account in leading logarithm approximation at this stage of the calculation by multiplying the wave functions  $\tilde{\Psi}(x, k_{ix}, b)$  with the exponential factor  $\exp[S(x, b, Q)]$  of Eq. (9).

The insertion of Eq. (15) and the use of the definition Eq. (16) leads to the factorized formula

$$\begin{aligned} M_{fi}(s, t) &= \frac{i}{(2\pi)^5} \frac{1}{2^5 Q^3 \sin \theta} \int_0^1 \frac{dx}{x^2 x'^2} \int db \int \sum_{i=1}^4 dk_{ix} \exp[-4 S(x, b, Q)] \\ &\times \left\{ \tilde{\Psi}_S^*(x, k_{4x}, b) \tilde{\Psi}_S^*(x, k_{3x}, b) \hat{M}_{qq;qq}(x, \hat{s}, \hat{t}) \hat{M}'_{SS;SS}(x, \hat{s}', \hat{t}') \tilde{\Psi}_S(x, k_{2x}, b) \tilde{\Psi}_S(x, k_{1x}, b) \right. \\ &\quad \left. + \tilde{\Psi}_S^*(x', k_{4x}, b) \tilde{\Psi}_S^*(x, k_{3x}, b) \hat{M}_{qS;qS}(x, \hat{s}, \hat{t}) \hat{M}'_{Sq;Sq}(x, \hat{s}', \hat{t}') \tilde{\Psi}_S(x', k_{2x}, b) \tilde{\Psi}_S(x, k_{1x}, b) \right\} \quad (17) \end{aligned}$$

for the helicity amplitude. Note that it is the inclusion of transverse momenta in the calculation which provides the key to derive the factorized formula. This is based on the simple fact that the Fourier transform of a convolution integral factorizes. Furthermore, the gluonic corrections are treated such that they are described by exponential factors to the wave

functions, which do not destroy the factorization.<sup>1</sup>

To perform the integrations over transverse momenta  $k_{xi}$  and  $k_{yi}$ , the latter contained in the definition of the  $\tilde{\Psi}_S(x, k_{ix}, b)$ , an ansatz for the wave functions has to be made. Here, the choice

$$\Psi_S(x, \vec{k}_\perp) = f_S \phi_S(x) \Sigma(x, \vec{k}_\perp) \quad (18)$$

is used where

$$\Sigma(x, \vec{k}_\perp) = 16\pi^2 \beta^2 g(x) \exp \left[ -g(x) \beta^2 k_\perp^2 \right] \quad \text{and} \quad g(x) = 1 \quad \text{or} \quad 1/xx' \quad . \quad (19)$$

The transverse momentum dependence is modeled as a simple Gaussian, where the case  $g(x) = 1$  assumes factorization of longitudinal and transverse degrees of freedom and the case  $g(x) = 1/(xx')$  is inspired by harmonic oscillator wave functions transformed to the light-cone, which have been conjectured to describe meson wave functions [27]. Correspondingly two DA's are used in the form

$$\phi_A(x) = N_A xx'^3 \exp \left[ -\beta^2 \left( \frac{m_q^2}{x} + \frac{m_S^2}{x'} \right) \right] \quad \text{for} \quad g(x) = 1/xx' \quad (20a)$$

$$\phi_B(x) = N_B xx'^3 \quad \text{for} \quad g(x) = 1 \quad . \quad (20b)$$

The polynomial  $\sim xx'^3$  is the equivalent to the asymptotic DA  $\sim x_1 x_2 x_3$  in the pure quark picture and is related to the latter by integration over one degree of freedom. The values for  $N_A$  and  $N_B$  are fixed by the normalization condition  $\int \phi(x) dx = 1$ . The Gaussian ansatz for the  $k_\perp$ -dependence models the unknown, intrinsic (non-perturbative) transverse structure of the proton. Note that fixing the oscillator parameter  $\beta$  with a phenomenological input, like the root mean square (r.m.s.) of the transverse momentum,  $\langle k_\perp^2 \rangle$ , introduces a hadronization or confinement scale.

---

<sup>1</sup>As was shown in [7] the factorized form even holds for loop corrections, which can't be written as an exponential multiplying the wave functions (type II. in Fig. 2), when a suitable 'soft approximation' is used.

With the ansatz of Eq. (19) the transverse momentum integrations lead to

$$M_{fi}(s, t) = \frac{i 4\pi^3}{Q^3 \sin \theta} f_S^4 \int_0^1 \frac{dx}{x^2 x'^2} \int db \phi^4(x) \hat{M}(x, \hat{s}, \hat{t}) \hat{M}'(x, \hat{s}', \hat{t}') \\ \times \exp \left[ -\frac{b^2}{g(x)\beta^2} \right] \cdot \exp [-4 S(x, b, Q)] \quad . \quad (21)$$

Eq. (21) displays the two exponential suppression factors brought about by the intrinsic, non-perturbative transverse structure and by the perturbative ‘Sudakov’ corrections. Obviously, the borderline between both effects will not be clearcut in nature. Nevertheless, Eq. (21) indicates the point of view adopted in the present paper: The perturbative formula for the ‘Sudakov’ factor is taken literally even in regions where perturbative calculations are known to become invalid, i.e.  $1/b$  as low as  $\Lambda_{QCD}$ . The intrinsic transverse structure, represented by the Gaussian, gives a weight function for the probability of finding transverse distances in a proton. Configurations with large  $b$  values, corresponding to the soft regions mentioned above (i.e.  $1/b \rightarrow \Lambda_{QCD}$ ), have a tiny probability to be found. Hence, the error induced in the calculation by retaining incorrectly the perturbative ‘Sudakov’ formula in the very soft region is expected to be small.

It is instructive to take a closer look at the interplay of the both exponentials in Eq. (21). In Fig. 3 the Gaussian  $\exp(-b^2/4\beta^2)$  (i.e.  $g(x) = 1$ ) for the value  $\beta^2 = 1.389 \text{ GeV}^{-2}$  (see Sec. IV) and the ‘Sudakov’ factor  $\exp[-S(x = 0.5, b, Q)]$ , the latter for different values of  $\ln(s/s_0)$  with  $s_0 \equiv 1 \text{ GeV}^2$ , are shown for comparison. Clearly for large values of  $\ln(s/s_0)$  the ‘Sudakov’ factor dominates the product of both. Thus, the asymptotic behavior of the cross-section as estimated by the saddle-point approximation Eq. (11), i.e.  $d\sigma/dt \sim s^{-9.83}$  is not affected by the additional intrinsic transverse structure. However, in the region of  $\ln(s/s_0)$  smaller than  $\simeq 5 \text{ GeV}^2$  the Gaussian dominates the product of both exponentials. Hence, taking into account the intrinsic transverse structure, e.g. in the form of a  $Q$ -independent Gaussian as in the present work, damps the  $Q$ -dependence inferred by the ‘Sudakov’ factor at least in the region of presently available data.

Using the Feynman rules of the quark-diquark model the helicity amplitudes can be calculated. Only three of them are non-zero and get contributions from 4 diagrams of type

Fig. 1a and 2 diagrams of type Fig. 1b:

$$M_{\{\lambda\}}^{hadr.}(s, t) = \frac{i 4^4 \pi^5 f_S^4}{9 Q^3 \sin \theta} \int_0^1 \frac{dx}{x^2 x'^2} \int_{-\infty}^{\infty} db \exp \left[ -\frac{b^2}{g(x) \beta^2} \right] \exp [-4 S(x, b, Q)] \alpha_s(x^2 t) \alpha_s(x'^2 t) \\ \times \left\{ \phi^4(x) F_S^2(x'^2 t) P_{\{\lambda\}}^{(i)}(s, t) - 2 \phi^2(x) \phi^2(x') F_S(x^2 t) F_S(x'^2 t) P_{\{\lambda\}}^{(ii)}(s, t) \right\} , \quad (22)$$

where  $\{\lambda\}$  denote the three sets of helicities  $(+, +, +)$ ,  $(+, -, -)$ , and  $(-, +, -)$ . The expressions  $P_{\{\Lambda\}}^{(i)}$  and  $P_{\{\Lambda\}}^{(ii)}$  are explicitly given as

$$P_{+,+,+}^{(i)}(s, t) = \left( \frac{s(s-u)}{t^2} + \frac{s(s-t)}{u^2} - \frac{s^2}{ut} \right) ; \quad P_{+,+,+}^{(ii)}(s, t) = \left( \frac{su}{t^2} - \frac{st}{u^2} \right) \\ P_{+,-,+}^{(i)}(s, t) = \left( \frac{1}{3} \frac{u(s-t)}{ut} - \frac{u(s-u)}{t^2} \right) ; \quad P_{+,-,+}^{(ii)}(s, t) = \left( \frac{su}{t^2} \right) \\ P_{-+,-}^{(i)}(s, t) = \left( \frac{t(s-t)}{u^2} - \frac{1}{3} \frac{t(s-u)}{ut} \right) ; \quad P_{-+,-}^{(ii)}(s, t) = \left( \frac{st}{u^2} \right) . \quad (23)$$

Using these results the differential cross section

$$\left. \frac{d\sigma^{pp \rightarrow pp}}{dt} \right|_{\substack{Ldsh. \\ diquark}}(s, t) = \frac{1}{16\pi} \frac{1}{s(s-4m_p^2)} \frac{1}{4} \left\{ |M_{+,+,+}|^2 + |M_{+,-,+}|^2 + |M_{-+,-}|^2 \right\} . \quad (24)$$

has been calculated for a scattering angle of  $90^\circ$ .

#### IV. NUMERICAL RESULTS

Parameters for the quark-diquark wave functions are taken from [20]:  $Q_S = 3.22 \text{ GeV}^2$  and  $\beta^2 = 0.247 \text{ GeV}^{-2}$  and  $1.389 \text{ GeV}^{-2}$  for wave functions (20a) and (20b), respectively. These values for the oscillator parameter correspond to a r.m.s. transverse momentum,  $\langle k_\perp^2 \rangle^{1/2}$  of 600 MeV. The value for  $f_S = 73.85 \text{ MeV}$  has been fixed by fits to the data of electromagnetic form factors of the nucleons [20]; masses of  $m_q = 330 \text{ MeV}$  and  $m_S = 580 \text{ MeV}$  are used.

Soft end-point regions of integration over longitudinal momenta ( $x \rightarrow 0$  or  $1$ ) with corresponding singularities in the strong couplings and in the gluon propagators are avoided by the introduction of a cut-off parameter  $C$  and the condition

$$\xi \geq C \frac{\Lambda}{\sqrt{2Q}} \quad \text{for } \xi = x, x' . \quad (25)$$

Independence from the cut-off serves as an indication for the range of applicability of the formalism. In the region of small  $b$  values,  $b \leq 1/\sqrt{2}xQ$ , the Sudakov factor  $e^{-S(x,b,Q)}$  is set to unity, it's value at  $b = 1/\sqrt{2}xQ$ .

Results for ‘Landshoff’ contributions to the differential cross sections at  $90^\circ$  obtained with the wave function from Eqs. (18), (19), and (20a) are shown in Fig. 4. The dimensionless quantity  $R(s) = d\sigma/dt|_{90^\circ} \times 10^{-8} s^{10} s_0^{-8}$  is plotted, which should become constant according to the ‘dimensional counting rules’. Results obtained with wave function B are very similar in shape and magnitude to the results in Fig. 4. They are smaller by some per cent and the independence of the cut-off is shifted a bit to higher  $\ln(s/s_0)$ . Since differences are really tiny, a figure by its own for it may be dispensed with.

The rise of the curves at lower values of  $\ln(s/s_0)$  are caused by the  $Q$ -dependence of the cut-prescription and, more important, by the behavior of the phenomenological vertex functions  $F_S(Q^2)$ , which have not yet reached their asymptotic  $Q^{-2}$  behavior. The position of the maximum is predominantly determined by the value of the diquark parameter  $Q_S$ . The fallings of the curves are induced by the behavior of the strong coupling; the cross section is proportional to  $\alpha_s^4$ .

A comment about the experimental data should be made here: The data reveal roughly the expected scaling with  $s^{-10}$  modified by, as it seems to be, an oscillation about it. It has been speculated [28] that the data indeed do not show the beginning of an oscillation, but a two peak structure, with the second peak caused by diquark correlations in the proton. The present results confirm the existence of a bump, even roughly peaked in the energy region of interest. But the shape and magnitude of this bump clearly disfavors this explanation for the structure of the data.

A different explanation has been suggested some years ago. Ralston and Pire [29] concluded the existence of a phase, proportional to  $\ln(s/s_0)$ , from analyticity properties of gluonic corrections and fitted the coefficients to the data. Botts and Serman [7] showed that corrections of type II in Fig. 2, neglected in the present paper, cause imaginary parts in the ‘Sudakov’ functions. However, the resulting phase is proportional to the ratio



$\ln(s/s_0)/\ln(b\Lambda)$ , which approaches a constant in the region where the saddle-point approximation Eq. (11) is valid, because of the power law behavior of the saddle-point  $b_{sp} \sim s^{-0.35}$ . Although the derivation of the phase from corrections of type II in Fig. 2 is beyond the scope of this paper, a comment can be made about this problem: The inclusion of the intrinsic transverse structure, neglected in previous papers, reconciles the  $s$ -dependence of the phase in the region  $\ln(s/s_0) \leq 5$ . Here, the Gaussian damps the ‘Sudakov’ factor and the dominantly contributing  $b$ -region is almost  $s$ -independent.

The magnitude of the results in Fig. 4 is roughly by a factor of 10 below the experimental data, but it is definitely not suppressed by many order of magnitudes as has been presumed before [2]. In this sense the result is an independent confirmation of the observations Botts made in the pure quark picture [8]. At  $\ln(s/s_0) = 5$  the results in [8] vary in the range of  $R = 0.07 \dots 9$  depending on the chosen distribution amplitude and the value of the cut-off. This is in accordance with the range of  $R = 0.5 \dots 1.5$  found in the present calculation in the framework of the quark-diquark model. The largest uncertainty in the magnitude of the results is caused by the normalization of the wave functions. The value  $f_S = 73.85$  MeV is taken from fits to the electromagnetic form factors of the nucleons [20]. These have been done without assuming a concrete  $k_\perp$ -dependence, what leads to a freedom to vary  $f_S$  in a limited range. Assuming a concrete  $k_\perp$ -dependence, like the Gaussian in the present case, fixes the relation between  $f_S, \langle k_\perp^2 \rangle$  and  $P_{qS}$ , the probability to find a proton as a system of a quark and a scalar diquark. The presently used values of  $\langle k_\perp^2 \rangle^{1/2}$  and  $f_S$  correspond to  $P_{qS} \simeq 1$ . Constraining, for example, this probability to be  $P_{qS} = 0.5$  would change  $f_S$  by a factor of 1/2 and correspondingly change the cross section by a factor of 1/16. These considerations may indicate that the lacking knowledge about the non-perturbative wave functions easily induces uncertainties of one order of magnitude.

Comparison to data is, somehow, ambiguous because the results show strong cut-off dependence in the region of the data. Independence of the cut-off and therefore applicability of the formalism is reached for  $\ln(s/s_0) \simeq 6$  (i.e.  $s \simeq 400$  GeV<sup>2</sup>). This has to be contrasted with a value of  $\ln(s/s_0) \simeq 8$  (i.e.  $s \simeq 3000$  GeV<sup>2</sup>) given in [8]. Thus the hope of improving

the applicability down to lower values of  $s$  by using the quark-diquark model is fulfilled.

A further improvement of applicability will surely be obtained by taking into account also the transverse momenta in the hard scattering amplitudes itself, which have been neglected up to now. Thus, the strategy of [10,11], developed for form factors, could be adopted; i.e. to characterize soft regions by both, small  $x$  and small transverse momenta (or large  $b$  values). These regions are suppressed by the ‘Sudakov’ factor. The transfer of this concept to the present case of proton-proton scattering is not straightforward, because the inclusion of transverse momenta in the gluon propagators would destroy the factorized form of Eq.(21). What can safely be done to improve the applicability of the calculation, is the replacement of the arguments of the strong coupling in the form

$$\alpha_s(x^2t) \rightarrow \alpha_s(\max(x^2t, 1/b^2)) \quad \alpha_s(x'^2t) \rightarrow \alpha_s(\max(x'^2t, 1/b^2)) \quad . \quad (26)$$

Such, the largest scale in each independent hard process determines the strength of the coupling. For vanishingly small  $x, x'$  the transverse scale takes over.

Results with these prescriptions, Eq. (26) are displayed in Fig. 5 in comparison with the curves from Fig. 4. Evidently they coincide asymptotically. For small values of  $\ln(s/s_0)$  the modified version lies a bit below the results obtained with a cut-off  $C = 1.1$ . This effect is readily explained by noting that the arguments of the coupling have become smaller on an average. It’s worth emphasizing that the modified result (i.e. the solid line in Fig. 5) is derived entirely without a cut-off (or  $C = 0$ ). On the contrary, results of calculations without the replacement Eq. (26) diverge for  $C \leq 1$ . The reliability of the modified calculation, and thus the effectivity of ‘Sudakov’ suppression of soft regions, can be checked by testing the portion which has been obtained with reasonable small values of the strong coupling, say  $\alpha_s \leq 0.5$ . It turns out that at  $\ln(s/s_0) = 1.5$  52% and at  $\ln(s/s_0) = 3$  even 84% of the full result fulfill this criterion.

Clearly the replacement Eq. (26) does not substitute a calculation with all the transverse momentum dependence taken into account in the hard scatterings. But results are quite encouraging that such a, still lacking, more complete calculation will render the formalism

reliable down to the energy range of the data.

## V. CONCLUSIONS

It has been emphasized that transverse momenta are the key of understanding for multiple, independent scattering processes with respect to factorization and their scaling behavior. The present calculation of ‘Landshoff’ contributions to the elastic proton-proton scattering at wide angles in the framework of the quark-diquark model is an independent confirmation of observations made before [8] in the pure quark picture. The magnitude of ‘Landshoff’ contributions is small, but definitely not suppressed by many orders of magnitude and, therefore, a priori not negligible. The main uncertainties in the calculation stem from our incomplete knowledge about non-perturbative wave-functions and the applicability of the calculation, as indicated by cut-off independence, is beyond the range of experimental access. It has been shown that the phenomenological quark-diquark model, as additional assumption to the hard scattering picture, improves the range of applicability of the perturbative calculations substantially down to smaller values of  $s$ , but still outside the energy region of experimental data.

A way out of this problem by taking into account transverse momenta scales, at least in the argument of the strong coupling, has been discussed and numerically tested. The results clearly indicate that an extension of the HSP by taking into account transverse momenta consistently (i.e. also in the hard scattering amplitudes) will lead to self-consistency of the perturbative calculation and, thus, will improve the reliability of the results down to even very small values of  $s$ .

## ACKNOWLEDGMENTS

I would like to thank J. Botts, T. Gousset, B. Pire and J.P. Ralston for clarifying discussions and P. Kroll for invaluable advice and careful corrections.

## REFERENCES

- [1] S.J. Brodsky, G.R. Farrar, Phys. Rev. D11 (1975) 1309
- [2] G.P. Lepage, S.J. Brodsky, Phys. Rev. D22 (1980) 2157
- [3] A.V. Efremov, A.V. Radyushkin, Phys. Lett. B94 (1980) 245
- [4] N. Isgur, C.H. Llewellyn Smith, Phys. Rev. Lett. 52 (1984) 1080;  
N. Isgur, C.H. Llewellyn Smith, Nucl. Phys. B317 (1989) 526;  
N. Isgur, C.H. Llewellyn Smith, Phys. Lett. B217 (1989) 535
- [5] F.M. Dittes, A.V. Radyushkin, Sov. J. Nucl. Phys.34(1981)293;  
A.V. Radyushkin, Nucl. Phys. A532 (1991) 141c;  
A.V. Radyushkin, preprint CEBAF-TH-93-12, (1993)
- [6] P.V. Landshoff, Phys. Rev. D10 (1974) 1024
- [7] J. Botts, G. Sterman, Nucl. Phys. B325 (1989) 62
- [8] J. Botts, Nucl. Phys. B353 (1991) 20
- [9] V. Sudakov, Zh. Eksp. Teor. Fiz. 30 (1956) 87
- [10] H.N. Li and G. Sterman, Nucl. Phys. B381 (1992) 129
- [11] H.N. Li, Phys. Rev. D48 (1993) 4243
- [12] R. Jakob, P. Kroll, Phys. Lett. B315 (1993) 463
- [13] J. Bolz et al., preprint WU-B-94-06, RUB-TPH-01/94, Wuppertal (1994)
- [14] T. Hyer, Phys. Rev. D47 (1992) 3875
- [15] C. Coriano, H.N. Li, Phys. Lett. B309 (1993) 409
- [16] A.R. Zhitnitsky, preprints SMU-HEP-93-25, Dallas (1993),  
and SMU-HEP-94-01, Dallas (1994)

- [17] T. Gousset, B. Pire, preprint DAPNIA/SPhN-94-09, Saclay (1994)
- [18] P. Kroll, Proceedings of the Adriatico Research Conference on ‘Spin and dynamics in nuclear and particle physics’, Triest (1988); P. Kroll, M. Schürmann, W. Schweiger, Z. Phys. A338 (1991) 339 and A342 (1992) 429; P. Kroll, M. Schürmann, W. Schweiger, Int. J. Mod. Phys. A6 (1991) 4107
- [19] P. Kroll, T. Pilsner, M. Schürmann, W. Schweiger, Phys. Lett. B316 (1993) 546
- [20] R. Jakob, P. Kroll, M. Schürmann, W. Schweiger, Z. Phys. A347 (1993) 109
- [21] S.J. Brodsky, G.R. Farrar, Phys. Rev. Lett. 31 (1973) 1153;  
V.A. Matveev, R.M. Muradyan, A.V. Tavkhelidze,  
Lett. Nuovo Cimento 7 (1973) 719
- [22] J.M. Cornwall, G. Tiktopoulos, Phys. Rev. D13 (1976) 3370
- [23] V.V. Belokurov, N.I. Ussyukina, Phys. Lett. 94B (1980) 251;  
H.D. Dahmen, F. Steiner, Z. Phys. C11 (1981) 247
- [24] J.C. Collins, Phys. Rev. D22 (1980) 1478;  
J.C. Collins, D.E. Soper, Nucl. Phys. B193 (1981) 381 and Nucl. Phys. B194 (1982) 445
- [25] A. Sen, Phys. Rev. D24 (1981) 3281
- [26] A.H. Mueller, Phys. Rep. 73 (1981) 237
- [27] G.P. Lepage, S.J. Brodsky, T. Huang and P.B. Mackenzie, Banff Summer Institute, Particles and Fields 2, S. 83, A.Z. Capri and A.N. Kamal (eds.), 1983
- [28] V.V. Anisovich, et al., preprint St. Petersburg (1992);  
Proceedings of the Intern. Workshop on Quark Cluster Dynamics, K. Goeke, P. Kroll, H.-R. Petry (eds.), Bad Honnef (1992)
- [29] J.P. Ralston, B. Pire, Phys. Rev. Lett. 49 (1982) 1605;

B. Pire, J.P. Ralston, Phys. Lett. 117B (1982) 233

[30] J. Bystricki, F. Lehar, Nucleon-Nucleon Scattering Data, Fachinformationszentrum  
Karlsruhe (1978)

## FIGURES

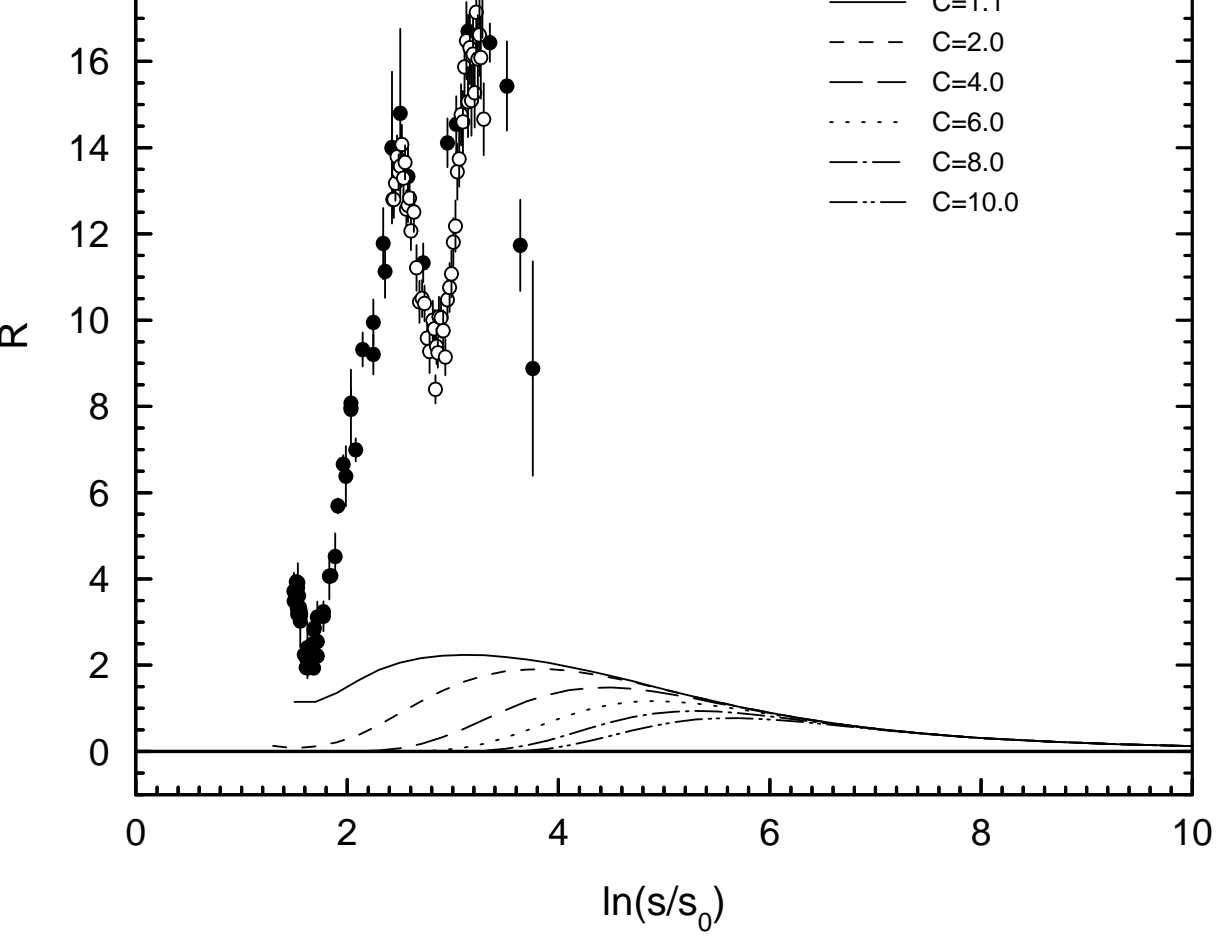
FIG. 1. Types of diagrams contributing to elastic proton-proton scattering at wide angles via the ‘Landshoff’ mechanism. Protons are considered as quark-diquark systems; double lines indicate the diquarks.

FIG. 2. One-loop gluonic corrections to the diagrams of Fig. 1. Type I. corrections may be factorized into the wave functions. Type II. corrections are non-factorizable.

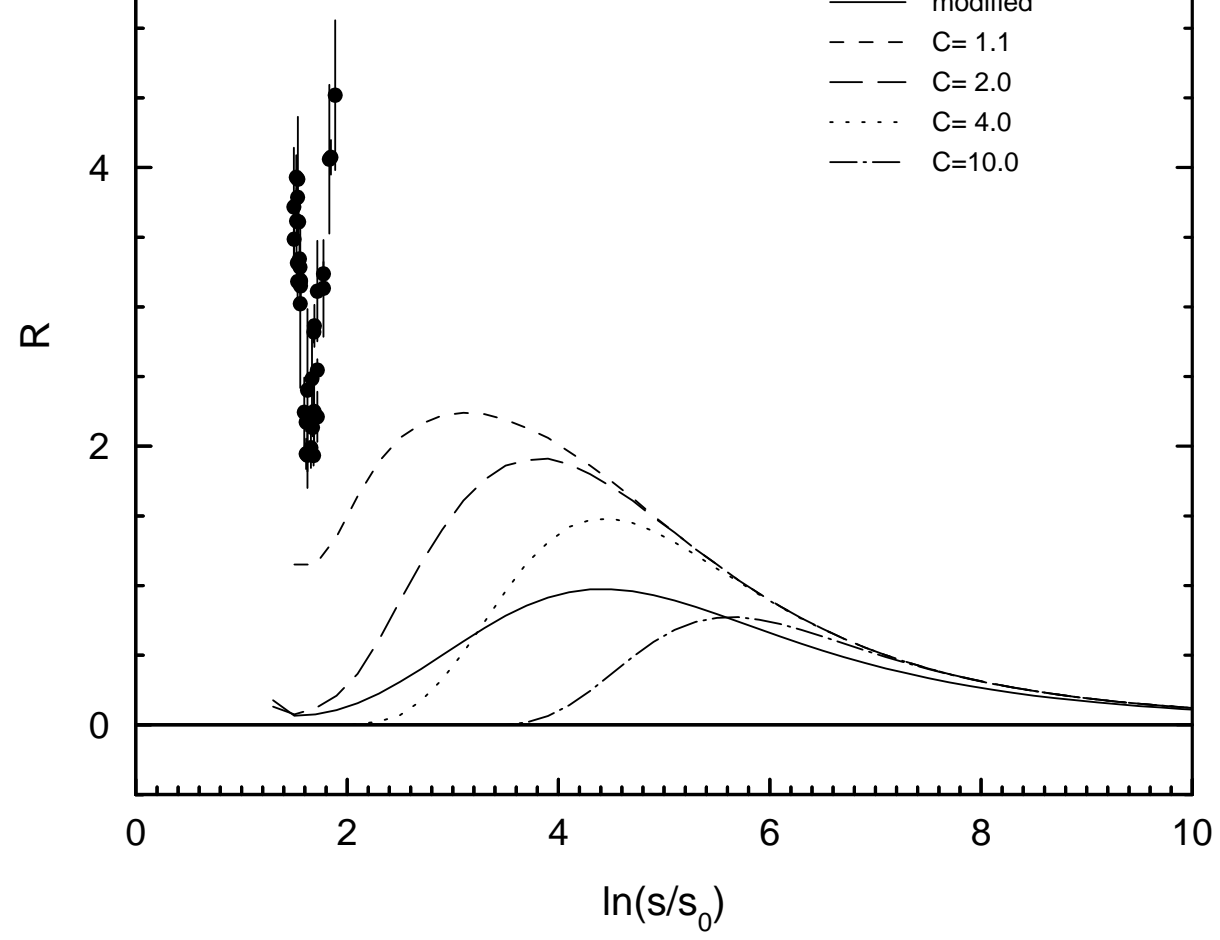
FIG. 3. Sudakov factor of Eq. (9) for  $x = 0.5$  and different values of  $\ln(s/s_0)$  with  $s_0 \equiv 1 \text{ GeV}^2$  (dashed and dashed-dotted lines). For comparison the Gaussian  $\exp(-b^2/4\beta^2)$  caused by the intrinsic transverse momentum dependence is also shown (solid line).

FIG. 4. Elastic Proton-proton scattering at  $90^\circ$ . The dimensionless quantity  $R(s) = d\sigma/dt|_{90^\circ} \times 10^{-8} s^{10} s_0^{-8}$  obtained with wave function (20a) is plotted against  $\ln(s/s_0)$ . Data are taken from the data compilation [30].

FIG. 5. Comparison of modified calculation, Eq. (26), with the cut-off method (cf. Fig. 4). Both calculations are done with wave function (20a).

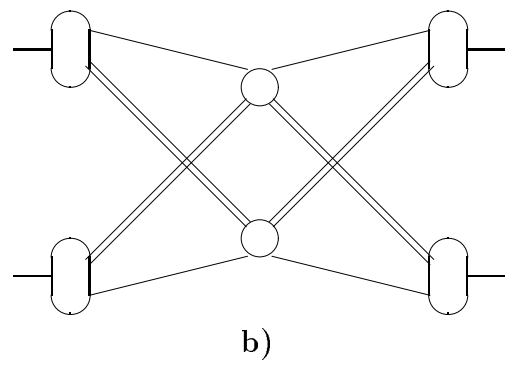
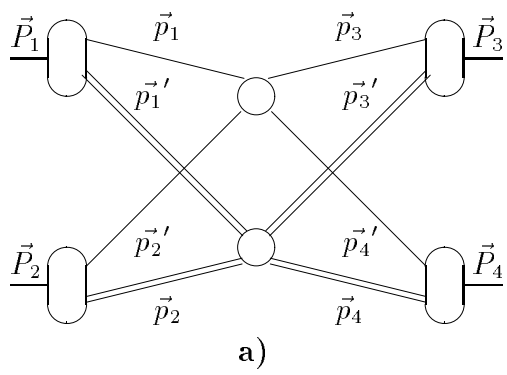






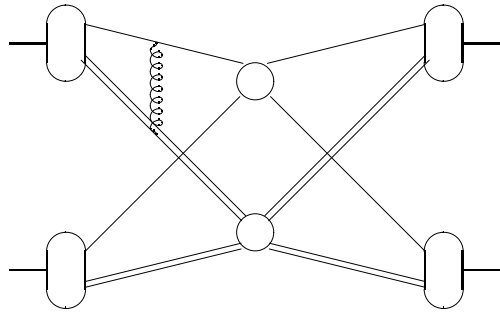
This figure "fig1-1.png" is available in "png" format from:

<http://arxiv.org/ps/hep-ph/9406250v1>

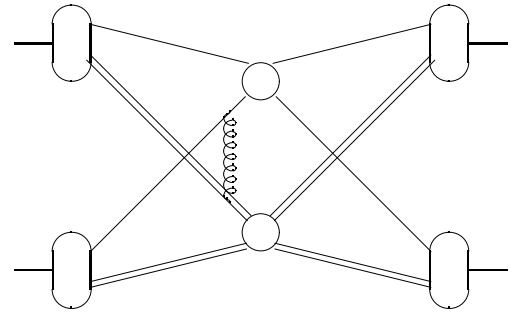


This figure "fig1-2.png" is available in "png" format from:

<http://arxiv.org/ps/hep-ph/9406250v1>



**a)I.**



**a)II.**

This figure "fig1-3.png" is available in "png" format from:

<http://arxiv.org/ps/hep-ph/9406250v1>

This figure "fig1-4.png" is available in "png" format from:

<http://arxiv.org/ps/hep-ph/9406250v1>

This figure "fig1-5.png" is available in "png" format from:

<http://arxiv.org/ps/hep-ph/9406250v1>



